

Temperature dependence of the photoluminescence properties of colloidal CdSe/ZnS core/shell quantum dots embedded in a polystyrene matrix

D. Valerini, A. Cretí,* and M. Lomascolo[†]*Istituto per la Microelettronica e i Microsistemi, Via Per Arnesano 73100 Lecce, Italy*

L. Manna, R. Cingolani, and M. Anni

National Nanotechnology Laboratory (NNL) of INFM, Dipartimento di Ingegneria dell'Innovazione, Università degli Studi di Lecce, Via per Arnesano 73100 Lecce, Italy

(Received 17 December 2004; revised manuscript received 25 February 2005; published 13 June 2005)

We report on the temperature dependence of the photoluminescence (PL) spectrum and of the PL relaxation dynamics for colloidal CdSe/ZnS core/shell quantum dots (QDs) embedded in an inert polystyrene matrix. We demonstrate that the confinement energy in the QDs is independent of the temperature. The coupling with both acoustic and optical phonons is also studied. Quantum confinement results in a strong increase of the exciton-acoustic-phonon coupling constant, up to $71 \mu\text{eV/K}$, and in a reduced exciton-longitudinal-optical (LO)-phonon coupling constant, down to 21 meV, with respect to bulk CdSe. In addition, we demonstrate that the main nonradiative process that limits the quantum efficiency of the QD at room temperature is the thermal escape from the dot assisted by scattering with four LO phonons. Thermally activated trapping in surface states is also observed at low temperature, with an activation energy of about 15 meV.

DOI: 10.1103/PhysRevB.71.235409

PACS number(s): 78.66.Qn, 78.67.Bf, 78.47.+p, 78.55.Et

I. INTRODUCTION

In the past few years, colloidal semiconductor quantum dots (QDs) have demonstrated excellent properties for applications to light-emitting diodes (LEDs),^{1,2} optically pumped lasers,³ photovoltaic cells,⁴ telecommunications,⁵ and in biomedicine.⁶ Synthesis techniques of colloidal QDs allow the realization of samples with low size dispersion [even $\leq 5\%$ (Ref. 7)] and high quantum yield [in the range 50–80 % (Refs. 8 and 9)]. However, in order to use colloidal quantum dots as active materials in devices, thin films of nanocrystals, typically synthesized in solutions, have to be realized. To date, close-packed QD superlattices¹⁰ have been realized, as well as hybrid organic-inorganic blends with active polymers.¹¹ Composites of nanocrystals with polymers can provide materials that allow the processability and chemical tailorability of several conjugated polymers (for example, good film-forming properties) but that have QDs as active materials. A detailed knowledge of the radiative and nonradiative relaxation processes of QDs in polymeric matrixes is therefore fundamental for future applications of colloidal QDs in hybrid organic-inorganic photonic and optoelectronic devices.

In this work, we investigate the photoluminescence (PL) properties of colloidal CdSe/ZnS core/shell QDs immobilized in an inert polystyrene (PS) matrix, as a function of the sample temperature, in the range 45–295 K. We demonstrate that the confinement energy in the dots is almost independent of the temperature. In addition, we have investigated the exciton coupling with both acoustic and optical phonons. This study shows an increase of the acoustic-phonon coupling constant up to $71 \mu\text{eV/K}$ and a reduced optical-phonon coupling constant, down to 21 meV, with respect to the bulk CdSe. A longitudinal-optical (LO)-phonon energy of about 24.5 ± 2.0 meV is determined, which is similar to previously

reported values for CdSe nanocrystals. We also demonstrate that, under our excitation conditions, the main nonradiative process is thermal escape from the dot assisted by scattering with four LO phonons. Moreover, evidence of thermally activated carrier trapping in superficial states is observed, with an activation energy of about 15 meV.

II. EXPERIMENT

The CdSe/ZnS core/shell QDs were prepared in analogy of the method described in Ref. 8 and were dissolved in a chloroform solution, while the polystyrene was purchased by Sigma-Aldrich and used without any further purification. The PS-QD films were realized by spin coating a PS-QD blend in a chloroform solution. The concentration of the dots in the blend was determined from the absorption spectrum of the QDs in a chloroform solution by the Lambert-Beer law (with values of the molar extinction coefficient taken from the literature^{12–14}). The dots/polymer relative concentration in the sample is about 8.3×10^{-2} dots/molecule. The samples were excited by the 2 ps pulses of the second harmonic ($\lambda=380$ nm) of a mode-locked (82 MHz) Spectra Physics Tsunami Ti-sapphire laser. The PL was then dispersed by a TRIAX 320 mm monochromator and detected by a Jobin-Yvon Si-CCD. The PL relaxation dynamics were obtained by a monochromator (0.24 m focal length) coupled with a Hadland Photonics Imacon 500 streak-camera. The temporal resolution was about 20 ps. The PL measurements were performed under vacuum, and the film temperature was varied from 45 K to room temperature (295 K) in steps of 20 K. The QD average radius \bar{R} and size dispersion δR , estimated from the TEM images and from the absorption spectra¹⁵ in a chloroform solution, are $\bar{R}=25$ Å and $\delta R=10\%$, respectively.

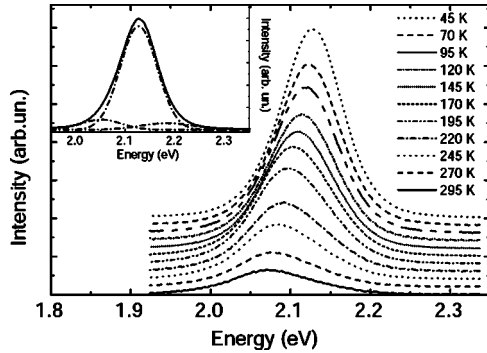


FIG. 1. PL spectra as a function of the temperature; the spectra are vertically translated for clarity. Inset: PL spectrum at $T=45$ K (continuous line) and the three best-fit Gaussians (dot-dashed lines).

III. RESULTS AND DISCUSSION

The PL spectra of the film as a function of the temperature are reported in Fig. 1. The emission spectra show a small shoulder in the high-energy tail (visible also in the room-temperature spectra of solutions, not reported) and a low-energy shoulder, not present in the solution spectra. To take into account these features, we fitted the PL curve at each temperature with a sum of three Gaussians (as an example, see the inset of Fig. 1). The high-energy PL resonance can be ascribed to the presence, in our colloidal QDs sample, of CdSe cores not covered, or partially covered by the ZnS shell, emitting at higher energy with respect to the CdSe/ZnS core/shell dots.⁸ The low-energy PL resonance, not present in the solution spectra, can be ascribed to the emission from the largest dots in the size distributions enhanced by Förster resonant energy transfer (FRET) from smaller dots.¹⁶ The low relative intensity of this low-energy emission with respect to the main PL resonance (due to the emission from the average dimension dots) clearly indicates that FRET is present only in a few regions of the sample, while most of the emission comes from single dots isolated in the matrix.

As the sample temperature is increased, the PL intensity decreases, the emission energy redshifts, and the spectra become broader, in qualitative agreement with the results obtained for CdSe/ZnS dots immobilized in a poly(lauryl methacrylate) (PLMA) matrix.¹⁷

The temperature dependence of the main PL resonance peak energy, which represents the energy gap of the average size dots, is reported in Fig. 2. The QD energy gap shows a redshift of about 54 meV as the temperature increases from 45 K to 295 K. The experimental data have been fitted to the Varshni relation,¹⁸ which gives the temperature dependence of the energy gap of bulk semiconductors,

$$E_g(T) = E_{g0} - \alpha \frac{T^2}{(T + \beta)}, \quad (1)$$

where E_{g0} is the energy gap at 0 K, α is the temperature coefficient, and the value of β is close to the Debye temperature θ_D of the material. The best-fit curve, with $\alpha = (3.2 \pm 0.2) \times 10^{-4}$ eV/K and $\beta = 220 \pm 30$ K, well reproduces the experimental data. These values are consistent with the

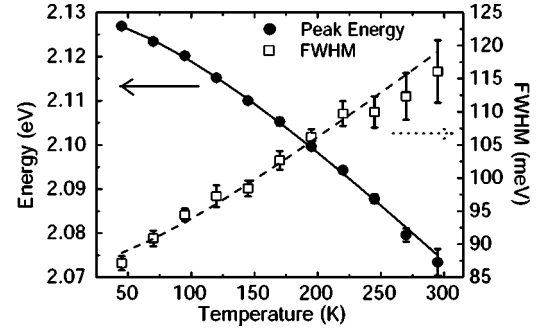


FIG. 2. PL peak energy (full dots) and FWHM (empty squares) as a function of the temperature. The lines are the best-fit curves as discussed in the text.

values known in the literature for bulk CdSe: $(2.8-4.1) \times 10^{-4}$ eV/K for α and $(181-315)$ K for θ_D (Ref. 19), thus demonstrating that the energy shift with temperature is due to the temperature-dependent band-gap shrinkage of the CdSe, while the confinement energies for the carriers are not dependent on the sample temperature. Such a result can be easily understood in a simple 3D potential-well picture with finite barrier. As the sample temperature increases, the barrier height changes, due to the different temperature dependence of the CdSe and the ZnS energy gap, and the potential well becomes larger, due to thermal expansion. Assuming for both the CdSe and the ZnS a bulk energy gap dependence,¹⁹ it is easy to calculate that the energy gap mismatch variation in the range 45–300 K is of the order of 20 meV, while the low-temperature value is about 1.99 eV. It is evident that such a small variation leads to negligible effects on the confinement energy. Concerning the dot size variation due to thermal expansion, assuming a linear thermal dilatation coefficient²⁰ of bulk CdSe (7.4×10^{-6} K⁻¹), a maximum radius variation of only 0.045 Å can be estimated, corresponding²¹ to an emission energy variation of about 0.5 meV, much lower than the observed shift.

The full width at half maximum (FWHM) Γ of the main PL resonance (see Fig. 2) continuously increases with the sample temperature. In order to have a deeper insight into the carrier-phonon scattering processes involved in the increasing broadening, we fitted the experimental data to the following relation, which describes the temperature dependence of the excitonic peak broadening in bulk semiconductors²² and which can be used for QDs:²³

$$\Gamma(T) = \Gamma_{\text{inh}} + \sigma T + \Gamma_{\text{LO}} (e^{E_{\text{LO}}/k_B T} - 1)^{-1}, \quad (2)$$

where Γ_{inh} is the inhomogeneous broadening, which is temperature-independent, and it is due to fluctuations in size, shape, composition, etc. of the nanocrystals. The last two terms represent the homogeneous broadening due to exciton-phonon interactions, σ is the exciton-acoustic-phonon coupling coefficient, Γ_{LO} represents the exciton-LO-phonon coupling coefficient, E_{LO} is the LO-phonon energy, and k_B is the Boltzmann constant. A good agreement between the experimental data and the best-fit curve is obtained for $\Gamma_{\text{inh}} = (85.5 \pm 0.7)$ meV, $\sigma = (71 \pm 9)$ $\mu\text{eV/K}$, $\Gamma_{\text{LO}} = (21 \pm 7)$ meV, and $E_{\text{LO}} = (24.5 \pm 2)$ meV.

The extracted value of σ is much higher than the values usually reported for bulk²⁴ CdSe, which are around $8 \mu\text{eV/K}$. This indicates a strong increase of the coupling with acoustic phonons, induced by the reduced dimensionality of the system. This result is in qualitative agreement with both theoretical^{25–27} and experimental studies^{24,28} performed on different semiconductor QDs. However, the obtained value is about two times larger than the theoretical value for an isolated CdSe dot of 25 \AA radius,^{25,29} calculated by taking into account the size dependence of the deformation potential coupling. This result can be ascribed to the presence of some additional dephasing process, probably induced by surface defects or trap states, which are expected to give important contribution to the homogeneous linewidth in the very small size regime.²⁹ A further contribution to the increased homogeneous broadening comes from the coupling between the QDs and the organic matrix, which has been already demonstrated to provide the main coherent confined acoustic-phonon damping route for InAs QDs in a PMMA matrix.³⁰ Concerning the scattering with optical phonons, the best-fit value of $\Gamma_{\text{LO}} \approx 21 \text{ meV}$ is considerably reduced with respect to the bulk value³¹ (about 100 meV). This result is also due to quantum confinement, as previously theoretically predicted²⁷ and experimentally observed.^{24,26} The strong quantum confinement is also expected to affect the phonon energy, due to mechanical boundary conditions³² and to the presence of surface phonons, with an energy smaller than the longitudinal phonons.³³ Both of these effects are size-dependent, as theoretically investigated³⁴ and experimentally observed from Raman spectra³³ for CdSe nanocrystals. The observed best-fit value of the LO energy $E_{\text{LO}} = 24.5 \pm 2.0 \text{ meV}$ is smaller than the bulk value of 26.1 meV (Ref. 19), and is in good agreement with the values expected from theory for a 25 \AA radius CdSe nanocrystal, which are in the range $23.8\text{--}26.0 \text{ meV}$ for the first four LO phonons.³⁴ Our result is also consistent with the E_{LO} values obtained from low-temperature Raman spectroscopy on CdSe nanocrystals of 22.5 \AA radius in polystyrene films³⁵ ($205 \text{ cm}^{-1} \approx 25.4 \text{ meV}$), in 26 \AA radius nanocrystals in a glass matrix³³ ($208.1 \text{ cm}^{-1} \approx 25.8 \text{ meV}$), and from low-temperature PL in 16 \AA radius CdSe nanocrystals in organic glass³⁶ ($200 \text{ cm}^{-1} \approx 24.8 \text{ meV}$).

In order to study the role of the different nonradiative processes in the relaxation of our QDs, we analyzed the temperature dependence of the PL intensity and of its relaxation dynamics.

The integrated PL intensity (see Fig. 3) weakly decreases as the temperature increases up to about 70 K , then a faster decrease is observed in the range $70\text{--}195 \text{ K}$ due to the activation of some nonradiative process, finally the intensity exponentially decreases above 195 K . This behavior suggests the presence in our system of two temperature-dependent nonradiative processes, which are activated in the range $70\text{--}195 \text{ K}$ and $195\text{--}295 \text{ K}$, respectively. In order to have a deeper insight into the nature of these processes, we modeled the emission intensity starting from a rate equation model. The possible processes that can lead to carrier relaxation in colloidal quantum dots are radiative relaxation, Auger non-radiative scattering,^{37,38} Förster energy transfer between dots of different dimensions, thermal escape from the dot,³⁹

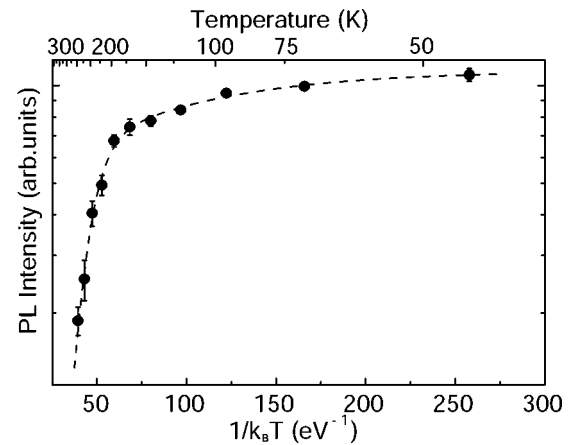


FIG. 3. Integrated emission intensity as a function of the sample temperature. The dashed line is the best-fit curve with the model described in the text.

and trapping in surface and/or defects states.^{40–42} In our experiment, the samples have been excited with an average laser power of about 1 mW with a spot diameter of about $100 \mu\text{m}$, corresponding to a photon fluence $j_p \approx 3 \times 10^{11} \text{ photons cm}^{-2}$ per laser pulse. The average number of excited electrons in each dot is given by $\langle N_0 \rangle = j_p \sigma_o$, where σ_o is the absorption cross section of the dot. When the quantum dot is pumped high above the energy gap, the absorption cross section can be expressed as $\sigma_o = \frac{4}{3} \pi |f|^2 \alpha_b R^3$, where α_b is the bulk absorption coefficient, R is the dot radius, and f is a coefficient accounting for local field effects.^{43,44} By fixing $\alpha_b = 1.6 \times 10^5 \text{ cm}^{-1}$ and $|f|^2 = 0.25$ (both at $h\nu = 3 \text{ eV}$),⁴⁴ we found $\sigma_o = 2.6 \times 10^{-15} \text{ cm}^2$ and $\langle N_0 \rangle \approx 7.7 \times 10^{-4} \ll 1$, which is small enough to neglect Auger scattering.⁴⁴ The energy transfer between dots can also be neglected because, as discussed previously, the sample emission mainly comes from isolated dots, and the emission of the largest dots, assisted by FRET, contributes less than 10% to the total emission intensity at all the investigated temperatures.

The considered rate equation for the carriers population n is then

$$\frac{dn}{dt} = g(t) - \frac{n}{\tau_{\text{rad}}} - \frac{n}{\tau_{\text{act}}} - \frac{n}{\tau_{\text{esc}}}, \quad (3)$$

where $g(t)$ is the generation term, $1/\tau_{\text{rad}}$ is the radiative recombination rate, and $1/\tau_{\text{esc}}$ is the thermal escape rate given by⁴⁵

$$\frac{1}{\tau_{\text{esc}}} = \frac{1}{\tau_0} (e^{E_{\text{LO}}/k_B T} - 1)^{-m}, \quad (4)$$

where $1/\tau_0$ is a fitting parameter acting as a weight for the probability of carrier-LO-phonon scattering, and m is the number of LO phonons involved in the process. The thermally activated process rate is given by

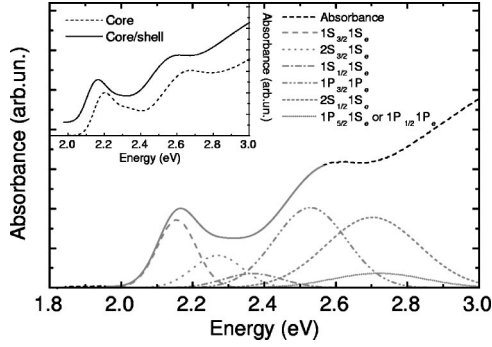


FIG. 4. Absorption spectrum of the CdSe/ZnS core shell quantum dots in chloroform solution. The gray lines are the best-fit curves of the first six excited states and the total fit. Inset: Comparison between the absorption spectrum of the core/shell and the core samples.

$$\frac{1}{\tau_{act}} = \frac{1}{\tau_a} e^{-E_a/k_B T}, \quad (5)$$

where E_a is the activation energy and $1/\tau_a$ is a fitting parameter acting as a weight for the probability of this process. The intensity of the PL emitted per unit time is given by

$$I_{PL}(t) = \frac{n(t)}{\tau_{rad}} = \frac{n_0}{\tau_{rad}} e^{-t/\tau}, \quad (6)$$

where n_0 is the initial carrier population and τ is the temperature-dependent PL decay time given by

$$\frac{1}{\tau} = \frac{1}{\tau_{rad}} + \frac{1}{\tau_{act}} + \frac{1}{\tau_{esc}}. \quad (7)$$

The integrated PL intensity is instead given by

$$I_{PL}(T) = \int_0^\infty I_{PL}(t) dt = \frac{n_0}{1 + \tau_{rad}/\tau_{act} + \tau_{rad}/\tau_{esc}}. \quad (8)$$

The experimental data have been fitted to Eq. (8) by fixing E_{LO} to 24.5 meV, as extracted from the temperature dependence of Γ . The best-fit curve excellently reproduces the

experimental data for $\tau_a/\tau_{rad}=0.82\pm 0.10$, $E_a=15\pm 5$ meV, $\tau_0/\tau_{rad}=0.026\pm 0.008$, and $m=4.4\pm 0.5$.

It has been recently demonstrated that in CdSe/ZnS quantum dots, thermally activated transfer from the dark $|J=2\rangle$ exciton state to the bright $|J=1\rangle$ exciton state takes place with an activation energy of a few meV.⁴⁶ In our experiment, we can exclude that E_a is the activation energy of this process as $|J=2\rangle \rightarrow |J=1\rangle$ should result in a PL blueshift and a PL intensity increase, which are both not observed. Moreover, the activation energy of $|J=2\rangle \rightarrow |J=1\rangle$ decreases with increasing dot radius. Therefore, in our dots the activation energy is expected to be smaller than 6 meV, which is the value found in 21 Å radius CdSe/ZnS QDs.⁴⁶ The obtained value for E_a suggests instead that the first thermally activated process is due to carrier trapping in surface states, probably at the dot/polymer interface.⁴⁷ The importance of the surface defects trapping is expected to increase with the increasing defects density. For this reason, the surface defects trapping is expected to be more evident in core nanocrystals, which are characterized by a higher surface defects density than core/shell nanocrystals.

In addition, the main nonradiative process, which limits the dot's quantum efficiency at room temperature, is the thermal escape from the dot assisted by the scattering with four LO phonons. This process, despite the higher activation energy, is characterized by a much higher rate, as evidenced by the much smaller value of τ_0 with respect to τ_a .

In order to understand the origin of the value of m , we estimated the energy values of the first six excited states from the absorption spectra of the CdSe/ZnS quantum dots in a chloroform solution. The spectra are reported in Fig. 4, together with a multi-Gaussian fit. In the fitting procedure, the inhomogeneous broadening Γ_i of each peak has been linked to the peak energy $\hbar\omega_i$ and the relative size dispersion δ_R through the relation¹⁵

$$\Gamma_i = 2\delta_R(\hbar\omega_i - E_g), \quad (9)$$

where E_g is the bulk CdSe energy gap.

The best-fit values of $\hbar\omega_i$ and Γ_i for the first six transitions, identified by following the attribution of Norris and Bawendi,²¹ are reported in Table I. It is evident from the

TABLE I. Peak energy and inhomogeneous broadening Γ of the absorption resonances of the core/shell and the core samples.

Transition	Peak energy core/shell (eV)	Γ core/shell (meV)	Peak energy core (eV)	Γ core (meV)
$1S_{3/2}1S_e$	2.155 ± 0.001	53.9 ± 0.2	2.196 ± 0.001	55.0 ± 0.3
$2S_{3/2}1S_e$	2.267 ± 0.001	69.2 ± 0.3	2.313 ± 0.001	69.4 ± 0.3
$1S_{1/2}1S_e$	2.368 ± 0.003	82.3 ± 0.5	2.408 ± 0.002	81.2 ± 0.5
$1P_{3/2}1P_e$	2.529 ± 0.001	103.8 ± 0.5	2.606 ± 0.002	105.7 ± 0.6
$2S_{1/2}1S_e$	2.703 ± 0.007	127 ± 1	2.803 ± 0.003	130.0 ± 0.7
$1P_{5/2}1S_e$ or	2.72 ± 0.04	129 ± 5	2.84 ± 0.04	135 ± 5
$1P_{1/2}1P_e$				

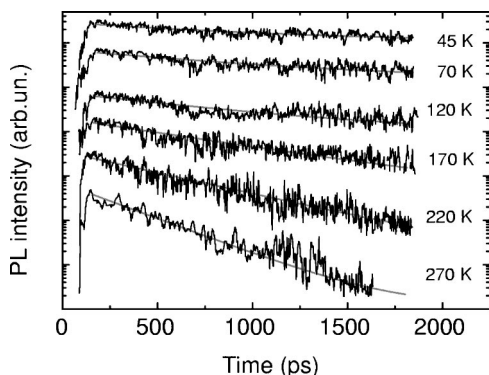


FIG. 5. Relaxation dynamics as a function of the sample temperature. The gray lines are the best-fit curves.

reported values that the energy difference between adjacent states is, for the first three transitions, in the range 101–112 meV, which is in good agreement with the energy of $4E_{LO}$. We can then conclude that the thermal escape is due to scattering with four LO phonons, as this energy matches the excited-states energy distance. For the other excited states, the increasing inhomogeneous broadening leads to an increasing spectral overlap, which allows phonon-assisted transitions between adjacent states, despite the increasing peak energy difference.

For this reason, the number of phonons assisting the thermal escape is expected to be dependent on the dot size. On the contrary, no strong effects of the shell overgrowth are expected on the thermal escape, as the shell growth only affects the peak energy of the absorption bands, but does not significantly affect the energy states separation. This is evident from the absorption spectrum of the CdSe core of our sample, reported in the inset of Fig. 4, which is just translated in energy with respect to the core/shell. A more quantitative analysis, with the same conclusions, can be done from the best-fit energy of the first six excited states of the core sample, reported in Table I.

In order to analyze the role of the nonradiative processes on the relaxation dynamics, we studied the PL relaxation dependence on the temperature. The PL relaxation dynamics (see Fig. 5) shows a monoexponential decay at all the investigated temperatures, and becomes faster at higher temperatures.

The decay time (see Fig. 6), as extracted from a fit of the experimental dynamics with Eq. (6), is slowly decreasing as the temperature increases up to about 70 K, then a faster decrease is observed in the range 70–195 K, and finally an exponential decrease for temperature higher than 195 K is observed.

The experimental decay time values are well reproduced by the best-fit curve to Eq. (7) for $\tau_{rad}=(1450\pm 50)$ ps,

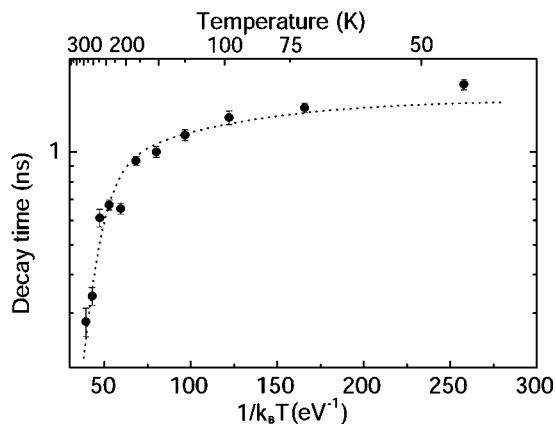


FIG. 6. PL decay time as a function of $1/k_B T$. The dotted line is the best-fit curve with the model described in the text.

$$\tau_a = (1200 \pm 150) \text{ ps} \approx 0.80 \tau_{rad}, \quad E_a = (15 \pm 4) \text{ meV}, \quad \tau_0 = (40 \pm 10) \text{ ps} \approx 0.027 \tau_{rad}, \quad \text{and } m = 4.1 \pm 0.5, \quad \text{while } E_{LO} \text{ has been fixed to } 24.5 \text{ meV.}$$

The value obtained for τ_{rad} is of the same order of magnitude previously encountered in nanocrystals,⁴⁸ while the values of the other parameters are in good agreement with those obtained from the analysis of the PL intensity temperature dependence, and confirm that thermal escape from the dots is assisted by scattering with four LO phonons, and it is the main nonradiative process for our quantum dots.

IV. CONCLUSIONS

In conclusion, we have analyzed the PL of colloidal CdSe/ZnS QDs embedded in a polystyrene inert matrix. The QDs energy gap in the PS matrix follows the same temperature behavior of bulk CdSe, demonstrating that the confinement energy is independent of the temperature. We demonstrated that the exciton-phonon coupling is instead strongly affected by quantum confinement, with an increase of the coupling with acoustic phonons and a decrease of the coupling with LO phonons. Finally, we analyzed the nonradiative processes involved in the relaxation of our QDs and we demonstrated that thermally activated carrier localization in surface states takes place with an activation energy of about 15 meV, while the main nonradiative process at high temperatures is thermal escape from the dot assisted by scattering with four LO phonons. These results clarify the properties of the relaxation processes involved in light emission from QDs in an inert matrix, and are important for future applications of colloidal QDs in hybrid organic-inorganic photonics and optoelectronic devices.

- *Also at Istituto Superiore Universitario Formazione Interdisciplinare ISUFI, Via Per Arnesano 73100 Lecce, Italy.
- †Corresponding author. Email address: mauro.lomascolo@imm.cnr.it
- ¹S. Coe, W. K. Woo, M. G. Bawendi, and V. Bulovic, *Nature (London)* **420**, 800 (2002).
 - ²N. Tessler, V. Medvedev, M. Kazes, S. H. Kan, and U. Banin, *Science* **295**, 1506 (2002).
 - ³V. I. Klimov, *Los Alamos Sci.* **28**, 214 (2003).
 - ⁴N. C. Greenham, X. Peng, and A. P. Alivisatos, *Phys. Rev. B* **54**, 17 628 (1996).
 - ⁵M. T. Harrison, S. V. Kershaw, M. G. Burt, A. L. Rogach, A. Kornowski, A. Eychmüller, and H. Weller, *Pure Appl. Chem.* **72**, 295 (2000).
 - ⁶X. Michalet, F. Pinaud, T. D. Lacoste, M. Dahan, M. P. Bruchet, A. P. Alivisatos, and S. Weiss, *Single Mol.* **2**, 261 (2001).
 - ⁷C. B. Murray, D. J. Norris, and M. G. Bawendi, *J. Am. Chem. Soc.* **115**, 8706 (1993).
 - ⁸B. O. Dabbousi, J. Rodriguez-Viejo, F. V. Mikulec, J. R. Heine, H. Mattoussi, R. Ober, K. F. Jensen, and M. G. Bawendi, *J. Phys. Chem. B* **101**, 9463 (1997).
 - ⁹P. Reiss, J. Bleuse, and A. Pron, *Nano Lett.* **2**, 781 (2002).
 - ¹⁰C. B. Murray, C. R. Kagan, and M. G. Bawendi, *Science* **270**, 1335 (1995).
 - ¹¹M. Anni, L. Manna, R. Cingolani, D. Valerini, A. Cretí, and M. Lomascolo, *Appl. Phys. Lett.* **85**, 4169 (2004).
 - ¹²W. W. Yu, L. Qu, W. Guo, and X. Peng, *Chem. Mater.* **15**, 2854 (2003); W. W. Yu *et al.*, *ibid.* **16**, 560(E) (2004).
 - ¹³A. Striolo, J. Ward, J. M. Prausnitz, W. J. Parak, D. Zanchet, D. Gerion, D. Milliron, and A. P. Alivisatos, *J. Phys. Chem. B* **106**, 5500 (2002).
 - ¹⁴C. A. Leatherdale, W. K. Woo, F. V. Mikulec, and M. G. Bawendi, *J. Phys. Chem. B* **106**, 7619 (2002).
 - ¹⁵V. I. Klimov, *J. Phys. Chem. B* **104**, 6112 (2000).
 - ¹⁶C. R. Kagan, C. B. Murray, and M. G. Bawendi, *Phys. Rev. B* **54**, 8633 (1996).
 - ¹⁷G. W. Walker, V. C. Sundar, C. M. Rudzinski, A. W. Wun, M. G. Bawendi, and D. G. Nocera, *Appl. Phys. Lett.* **83**, 3555 (2003).
 - ¹⁸Y. P. Varshni, *Physica (Amsterdam)* **34**, 149 (1967).
 - ¹⁹*Numerical Data and Functional Relationship in Science and Technology*, edited by K. H. Hellwege, Landolt-Börnstein, New Series, Group III, Vol. 17, Pt. B (Springer-Verlag, Berlin, 1982).
 - ²⁰H. Neumann, *Krist. Tech.* **15**, 849 (1980).
 - ²¹D. J. Norris and M. G. Bawendi, *Phys. Rev. B* **53**, 16 338 (1996).
 - ²²B. Segall, in *Proceedings of the IX Conference on the Physics of Semiconductors, Moscow, 1968*, edited by S. M. Ryvkin (Nauka, Leningrad, 1968), p. 425.
 - ²³L. G. Zhang, D. Z. Shen, X. W. Fan, and S. Z. Lu, *Chin. Phys. Lett.* **19**, 578 (2002).
 - ²⁴F. Gindele, K. Hild, W. Langbein, and U. Woggon, *J. Lumin.* **87–89**, 381 (2000).
 - ²⁵T. Takagahara, *Phys. Rev. Lett.* **71**, 3577 (1993).
 - ²⁶S. Nomura and T. Kobayashi, *Phys. Rev. B* **45**, 1305 (1992).
 - ²⁷S. Schmitt-Rink, D. A. B. Miller, and D. S. Chemla, *Phys. Rev. B* **35**, 8113 (1987).
 - ²⁸R. W. Schoenlein, D. M. Mittleman, J. J. Shiang, A. P. Alivisatos, and C. V. Shank, *Phys. Rev. Lett.* **70**, 1014 (1993).
 - ²⁹T. Takagahara, *J. Lumin.* **70**, 129 (1996).
 - ³⁰G. Cerullo, S. De Silvestri, and U. Banin, *Phys. Rev. B* **60**, 1928 (1999).
 - ³¹J. Voigt, F. Spielgelberg, and M. Senoner, *Phys. Status Solidi B* **91**, 189 (1979).
 - ³²M. P. Chamberlain, C. Trallero-Giner, and M. Cardona, *Phys. Rev. B* **51**, 1680 (1995).
 - ³³Y. N. Hwang, S. H. Park, and D. Kim, *Phys. Rev. B* **59**, 7285 (1999).
 - ³⁴C. Trallero-Giner, A. Debernardi, M. Cardona, E. Menendez-Proupin, and A. I. Ekimov, *Phys. Rev. B* **57**, 4664 (1998).
 - ³⁵A. P. Alivisatos, T. D. Harris, P. J. Carrol, M. L. Steigerwald, and L. E. Brus, *J. Chem. Phys.* **90**, 3463 (1989).
 - ³⁶M. G. Bawendi, P. J. Carroll, W. L. Wilson, and L. E. Brus, *J. Chem. Phys.* **96**, 946 (1992).
 - ³⁷M. Ghanassi, M. Schanne-Klein, F. Hache, A. Ekimov, and D. Ricard, *Appl. Phys. Lett.* **62**, 78 (1993).
 - ³⁸V. I. Klimov and D. W. McBranch, *Phys. Rev. B* **55**, 13 173 (1997).
 - ³⁹W. Yang, R. R. Lowe-Webb, H. Lee, and P. C. Sercel, *Phys. Rev. B* **56**, 13 314 (1997).
 - ⁴⁰V. I. Klimov, P. H. Bolivar, and H. Kurz, *Phys. Rev. B* **53**, 1463 (1996).
 - ⁴¹V. I. Klimov and D. W. McBranch, *Phys. Rev. Lett.* **80**, 4028 (1998).
 - ⁴²M. C. Nuss, W. Zinth, and W. Kaiser, *Appl. Phys. Lett.* **49**, 1717 (1986).
 - ⁴³D. Ricard, M. Ghanassi, and M. Schanneklein, *Opt. Commun.* **108**, 311 (1994).
 - ⁴⁴V. I. Klimov, D. W. McBranch, C. A. Leatherdale, and M. G. Bawendi, *Phys. Rev. B* **60**, 13 740 (1999).
 - ⁴⁵M. De Giorgi, C. Lingk, G. von Plessen, J. Feldmann, S. De Rinaldis, A. Passaseo, M. De Vittorio, R. Cingolani, and M. Lomascolo, *Appl. Phys. Lett.* **79**, 3968 (2001) and references therein.
 - ⁴⁶S. A. Crooker, T. Barrick, J. A. Hollingsworth, and V. I. Klimov, *Appl. Phys. Lett.* **82**, 2793 (2003).
 - ⁴⁷U. Banin, M. Bruchez, A. P. Alivisatos, T. Ha, S. Weiss, and D. S. Chemla, *J. Chem. Phys.* **110**, 1195 (1999).
 - ⁴⁸A. L. Efros, *Phys. Rev. B* **46**, 7448 (1992).